

Theory of quasiparticle vortex bound states in iron-based superconductors: Application to scanning tunneling spectroscopy of LiFeAs

Yan Wang,¹ Peter J. Hirschfeld,¹ and Ilya Vekhter²

¹*Department of Physics, University of Florida, Gainesville, Florida 32611, USA*

²*Department of Physics and Astronomy, Louisiana State University, Baton Rouge, Louisiana 70803-4001, USA*

(Received 2 November 2011; revised manuscript received 17 December 2011; published 24 January 2012)

The spectroscopy of vortex bound states can provide valuable information on the structure of the superconducting order parameter. Quasiparticle wave functions are expected to leak out in the directions of gap minima or nodes, if they exist, and scanning tunneling spectroscopy (STS) on these low-energy states should probe the momentum dependence of the gap. Anisotropy can also arise from band-structure effects, however. We perform a quasiclassical calculation of the density of states of a single vortex in an anisotropic superconductor, and show that if the gap itself is not highly anisotropic, the Fermi-surface anisotropy can dominate, preventing direct observation of superconducting gap features. This serves as a cautionary message for the analysis of STS data on the vortex state on Fe-based superconductors, in particular, LiFeAs, which we treat explicitly.

DOI: [10.1103/PhysRevB.85.020506](https://doi.org/10.1103/PhysRevB.85.020506)

PACS number(s): 74.70.Xa, 74.20.Rp, 74.25.Uv, 74.50.+r

Introduction. Four years after the discovery of iron-based^{1,2} high-temperature superconductors, the structure and symmetry of the gap function are still being debated. There is considerable experimental evidence that there is no universal gap shape,³⁻⁵ perhaps in part due to the electronic structure that combines small electron and hole pockets, leading to an “intrinsic sensitivity”⁶ to details. It is likely⁵ that in most cases the gap has A_{1g} symmetry, which, however, allows a continuous deformation from a full gap to that with nodes on the Fermi-surface (FS) sheets. Bulk experimental probes of the gap structure include specific heat and thermal conductivity oscillations in an external magnetic field,^{7,8} performed on the Fe(Te,Se) system⁹ and P-doped 122 family,¹⁰ respectively. In both systems the oscillation pattern was found to be consistent^{8,10-12} with an anisotropic gap with minima along the Γ -X axis (in the unfolded Brillouin zone), as predicted by spin fluctuation theories (see, e.g., Ref. 5).

The order parameter structure is also reflected in the local properties of inhomogeneous superconducting states. Inhomogeneities may arise due to impurities, and the resulting quasibound states in nodal superconductors have tails that “leak out” in the nodal directions,¹³ providing a signature of the amplitude modulation of the gap. The interpretation of these impurity states is complex: Disorder potentials can be of the order of electron volts, and hence relatively high-energy processes control the formation of such states, as well as their contribution to scanning tunneling spectroscopy (STS) images.¹⁴

Under an applied magnetic field, inhomogeneous superconductivity arises due to modulation of the order parameter in a vortex lattice, and bound states localized around the vortex cores appear. In this case, relevant energy scales are of the order of the gap or lower and the bound-state properties are determined by the shape of the gap and the band features near the Fermi surface. The decay length of the core states is of order of $\xi_{\text{BCS}} = v_F/\pi\Delta$, where v_F is the Fermi velocity and Δ is the gap amplitude. Consequently, variation of the gap with direction $\hat{\mathbf{k}}$ at the FS, $\Delta(\hat{\mathbf{k}}) \neq \text{const}$, directly influences the shape of the core states in real space, leading to the “tails” extending along nodes or minima. Since the decay of these states is exponential in distance ρ from the center of the vortex

(except along true nodes where it follows power laws), these tails are very clearly seen in local measurements, and can be used to probe the gap shape.¹⁵ The difficulties in interpretation exist in cuprates, where the coherence length is short and the cores may nucleate competing order (see, e.g., Ref. 16), but in most Fe-based superconductors (FeSC) these complications are less severe or absent over a wide range of experimentally tunable parameters.

On the other hand, a complex aspect of these latter systems arises due to their multiband nature. The directional dependence $v_F(\hat{\mathbf{k}})$ also affects the decay length of the core states, especially when combined with different gap amplitudes on different Fermi-surface sheets. In FeSC, the Fermi surface typically consists of two or three hole pockets and two electron pockets, as represented in the Brillouin zone corresponding to 1-Fe unit cell (see Fig. 1). The size and shape of these pockets varies considerably from family to family. A natural question is whether it is the normal-state band structure and the Fermi surface, or the order parameter shape that determine the salient features of the vortex core states as seen in experiment, and whether one can draw reliable conclusions about the directions of the gap nodes or minima based on the real-space structure of these states. This is the question we address in the current Rapid Communication.

The competition between the two effects has been explored numerically. For example, the sixfold pattern observed in 2H-NbSe₂ core states¹⁷ can be explained either by assuming a weak gap anisotropy or by using the angle-dependent density of states (DOS) around the Fermi surface.¹⁸ In pnictides it was argued both that the vortex core states are controlled by the order parameter shape¹⁹ and that the location of the peak in the DOS is determined by the proximity to the band edge in the electron or hole bands.²⁰ To gain qualitative insight into this issue we consider a simple model with both the order parameter and band anisotropy characteristic of the Fe-based superconductors, and find that, in the absence of strong nodes, the Fermi velocity anisotropy can dominate the real-space shape of the vortex core states. These states have been observed in STS experiments,²¹ albeit without the spatial resolution necessary to analyze the order parameter structure.

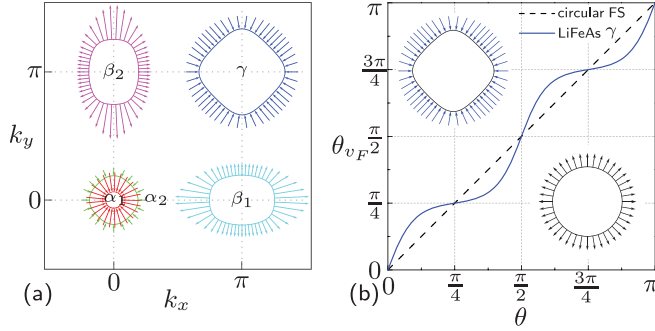


FIG. 1. (Color online) (a) Fermi surface of stoichiometric LiFeAs at $k_z = 0$ in the unfolded 1-Fe “effective” Brillouin zone from DFT. The Fermi velocities for different sheets are indicated by the arrows pointing to the higher $E(\mathbf{k})$. We label two inner hole pockets α_1, α_2 , one outer hole pocket γ , and two electron pockets β_1, β_2 . (b) The Fermi velocity direction θ_{v_F} vs the momentum \mathbf{k} azimuthal angle θ for the LiFeAs γ pocket and the circular Fermi surface (shown as insets).

We focus on the LiFeAs system, which is ideal for STS measurements due to its nonpolar surfaces. According to density functional theory (DFT) calculations,²² the Fermi surface of this material has three hole pockets and two electron pockets, (see Fig. 1). The outer hole pocket is large and quite square, according to both DFT results and angle-resolved photoemission spectroscopy (ARPES)²³ and de Haas–van Alphen (dHvA)²⁴ measurements. Both γ and α_2 pockets have small Fermi velocities and therefore large normal-state DOS. ARPES has identified superconducting leading edge gaps of order 1.5–2 meV for the hole pockets, and 3 meV for the electron pockets.²³ The London penetration depth data²⁵ and specific-heat measurements²⁶ ruled out the existence of gap nodes and were fit to models with two isotropic gaps with $(\Delta_1, \Delta_2) \simeq (3 \text{ meV}, 1.5 \text{ meV})$ and $(2 \text{ meV}, 0.5 \text{ meV})$, respectively. This suggests moderate gap anisotropy, which is not easily detected by the bulk measurements, but can substantially affect the real-space structure of the core states.

For circular Fermi surfaces the low-energy core bound states extend furthest in the direction of the smallest gap, but for realistic bands the Fermi velocity anisotropy plays a significant role. Since the cross sections of the β_1 and β_2 electron pockets rotate by a full 180° along the k_z direction, and since these gaps are larger, it is unlikely that these sheets contribute substantially to the spatial anisotropy. We therefore focus on the possible anisotropy of the gap on the hole Fermi surfaces. The most likely candidate for the anisotropic gap that dominates the low-energy vortex bound states is the γ pocket. The orbital content of this pocket is exclusively d_{xy} , and it couples only weakly to the primarily d_{xz} and d_{yz} electron pockets, which provide the main pairing weight in the conventional spin fluctuation approach.⁵ It is also nearly square, with weakly dispersive parallel surfaces oriented along the $[110]$ direction in the 1-Fe zone, and with significant variations of the Fermi velocity between the $[100]$ and $[110]$ directions. Hence we first neglect other FS sheets, and contrast the results obtained for the γ sheet alone with those for a single circular FS.

Model. We follow the approach of Ref. 27 that relied on the quasiclassical method for superconductivity,^{28–30} used previously to study vortex cores.³¹ The energy-integrated normal and anomalous Green’s functions $g(\mathbf{r}, \theta, i\omega_n)$ and $f(\mathbf{r}, \theta, i\omega_n)$ obey the coupled Eilenberger equations

$$\left[2 \left(i\omega_n + \frac{e}{c} \mathbf{v}_F \cdot \mathbf{A}(\mathbf{r}) \right) + i\hbar \mathbf{v}_F \cdot \nabla \right] f(\mathbf{r}, \theta, i\omega_n) = 2ig(\mathbf{r}, \theta, i\omega_n)\Delta(\mathbf{r}, \theta), \quad (1a)$$

$$\left[2 \left(i\omega_n + \frac{e}{c} \mathbf{v}_F \cdot \mathbf{A}(\mathbf{r}) \right) - i\hbar \mathbf{v}_F \cdot \nabla \right] \bar{f}(\mathbf{r}, \theta, i\omega_n) = 2ig(\mathbf{r}, \theta, i\omega_n)\Delta^*(\mathbf{r}, \theta), \quad (1b)$$

together with the normalization condition $g^2 + f\bar{f} = 1$. Here $\mathbf{A}(\mathbf{r})$ is the vector potential, \mathbf{v}_F is the Fermi velocity at the location at the Fermi surface labeled by θ , and $\omega_n = (2n + 1)\pi k_B T$ are fermionic Matsubara frequencies. The Fermi velocity $\mathbf{v}_F(\theta)$ is along the two-dimensional (2D) unit vector $\hat{\mathbf{k}}$ for the circular Fermi surface, and is computed for the γ band in LiFeAs using the Quantum ESPRESSO package,³² as in Ref. 33. In the low-field regime, we consider the problem of an isolated vortex and assume a separable momentum and coordinate dependence of the order parameter $\Delta(\rho, \hat{\mathbf{k}}) = \Delta_0 \Phi(\theta) \tanh(\rho/\eta_r \xi_0)$, where Δ_0 is the bulk gap value in the absence of the field and $\Phi(\theta)$ describes the gap shape on the Fermi surface, $\Phi_s = 1$, $\Phi_d = \sqrt{2} \cos 2\theta$, and $\Phi_{s,\text{ani}} = (1 - r \cos 4\theta)/\sqrt{1 + r^2/2}$ with $r = 0.3$, for the isotropic s -wave, nodal d -wave, and extended s -wave gaps, respectively.^{34,35} The coherence length is $\xi_0 = \hbar v_{F,\text{rms}}/\Delta_0$, where $v_{F,\text{rms}} = \sqrt{\langle |\mathbf{v}_F(\hat{\mathbf{k}})|^2 \rangle_{\text{FS}}}$, and the angle brackets $\langle \dots \rangle_{\text{FS}}$ denote the normalized average over the Fermi surface,

$$\langle \dots \rangle_{\text{FS}} = \frac{1}{\mathcal{N}} \oint_{\text{FS}} \frac{dk_{\parallel}}{|\mathbf{v}_F(\hat{\mathbf{k}})|} \dots = \int_0^{2\pi} \frac{d\theta}{2\pi} \tilde{\rho}(\theta) \dots, \quad (2)$$

where $\mathcal{N} \equiv \oint_{\text{FS}} \frac{dk_{\parallel}}{|\mathbf{v}_F(\hat{\mathbf{k}})|}$ and $\tilde{\rho}(\theta)$ is the angle-dependent density of states. The factor η_r accounts for the shrinking of core size at low temperature (Kramer-Pesch effect^{36,37}), and we set $\eta_r = 0.1$ corresponding to $T \sim 0.1T_c$. In a fully self-consistent calculation the gap anisotropy in momentum space will induce weak core anisotropy in real space,³⁸ which we ignore here since the effect is small even for nodal systems.³⁸

We solve Eq. (1) using the Riccati parametrization³⁹ and integrating along classical trajectories $\mathbf{r}(x) = \mathbf{r}_0 + x\hat{\mathbf{v}}_F$ to obtain the functions g and f at Matsubara frequencies. The local DOS (LDOS) is found after analytic continuation from the retarded propagators $N(\mathbf{r}, \omega) = N_0 \langle \text{Re } g^R(\mathbf{k}_F, \mathbf{r}, \omega + i\delta) \rangle_{\text{FS}}$. At each point $\mathbf{r} = (\rho, \phi)$ the LDOS is obtained by summation over the quasiclassical trajectories passing through \mathbf{r} . Each trajectory follows the direction of the Fermi velocity at a given point on the FS, $\hat{\mathbf{v}}_F(\hat{\mathbf{k}})$, and samples the gap $\Delta(\mathbf{r}(x), \hat{\mathbf{k}})$. The trajectories that sample regions of small order parameter contribute to the low-energy LDOS. This occurs if the trajectory either passes in the vicinity of the core where the order parameter is suppressed in real space, $\Delta(\rho) \ll \Delta_0$ (small impact parameter, dominant for isotropic gaps), or is along the direction where the gap has a node or a deep minimum in momentum space, $\Delta(\hat{\mathbf{k}}) \ll \Delta_0$ (dominant for nodal superconductivity).

The influence of the FS shape is then clear: The number of trajectories with a given impact parameter depends on the band structure. Denote the angle between $\hat{\mathbf{v}}_F$ and k_x axis as θ_{v_F} . For a circular FS, $\theta_{v_F} = \theta$, and quasiclassical trajectories in different directions θ_{v_F} are equally weighted in FS averaging. In contrast, for anisotropic cases, such as the square γ sheet in LiFeAs, large parts of the FS have the \mathbf{v}_F along the diagonals [see Fig. 1(b)], and therefore the average over the trajectories is heavily weighted toward that direction as well.

For an isotropic gap $\Delta(\hat{\mathbf{k}}) = \text{const}$, the largest contribution to the low-energy LDOS at $\mathbf{r} = (\rho, \phi)$ comes from the trajectories passing through the core, $\theta_{v_F} = \phi$ or $\phi + \pi$. For a cylindrical FS parameterized by angle θ this corresponds to two points since $\theta_{v_F} = \theta$. On an anisotropic FS, such as the γ pocket in LiFeAs, many different momentum angles θ correspond to $\theta_{v_F} \approx \pm \frac{\pi}{4}$, and quasiparticles from a large portion of the FS travel along these directions. For real-space direction $\phi = \frac{\pi}{4}$, all these trajectories sample the core region and contribute to the low-energy LDOS. For ϕ away from these directions these trajectories have a nonzero impact parameter and therefore small weight at low energies. For the extended s -wave gap model with $r > 0$ in the form factor $\Phi_{s,\text{ani}}$, this implies that the regions of large gap will be emphasized due to preferential directions of \mathbf{v}_F , and therefore the FS effects compete with the gap shape in determining the spatial profile of the vortex core states. Simply assuming that the direction of the smallest gap in \mathbf{k} space yields the orientation of the tails of the bound-state wave function need not be correct, and may be wrong with a strongly anisotropic Fermi surface.⁴⁰

Results. Figure 2 shows the zero energy density of states (ZDOS) of a circular Fermi surface [Figs. 2(a)–2(c)] and LiFeAs γ pocket [Figs. 2(d)–2(f)]. Comparing Figs. 2(a) and 2(d) for the isotropic gap, we see that the rotation symmetry of ZDOS in Fig. 2(a) is broken due to the anisotropy of γ pocket and Fermi velocity; at the same time the ZDOS still preserves the crystal fourfold symmetry. In the d -wave case, Fig. 2(b), for a circular Fermi surface, we recover well-known results for the ZDOS, including the double tails along the nodal directions forced by the vanishing of the bound-state wave function exactly along the 45° directions in the quasiclassical theory.³¹ While this feature remains, it becomes essentially invisible in the case of the square Fermi surface shown in Fig. 2(e), as the Fermi surfaces concentrate the quasiparticle trajectories even more in the nodal directions. Our primary results are now contained in Figs. 2(c) and 2(f). The extended- s state $\Phi_{s,\text{ani}}$ has been chosen deliberately to have gap minima along the 0° directions (along the Fe-Fe bond in the FeSC case). This is clearly visible in the case of an isotropic pocket, Fig. 2(c), as the tails, while not as well defined as in the true nodal case, extend clearly along these directions in real space. These directions rotate by 45° , however, when the same gap exists on the square LiFeAs γ pocket, as in Fig. 2(f). In fact, the ZDOS in Fig. 2(f) strongly resembles the structure observed by Hanaguri *et al.* in recent STS measurements on LiFeAs.⁴¹

The results in Fig. 2 strongly challenge the common interpretation of STS images of vortices, which assign gap minima to the directions of the extended intensity in real space. This is probably reasonable in the case of true nodes, as indicated by the d -wave examples shown, but fails if these minima are not sufficiently deep due to the competition with

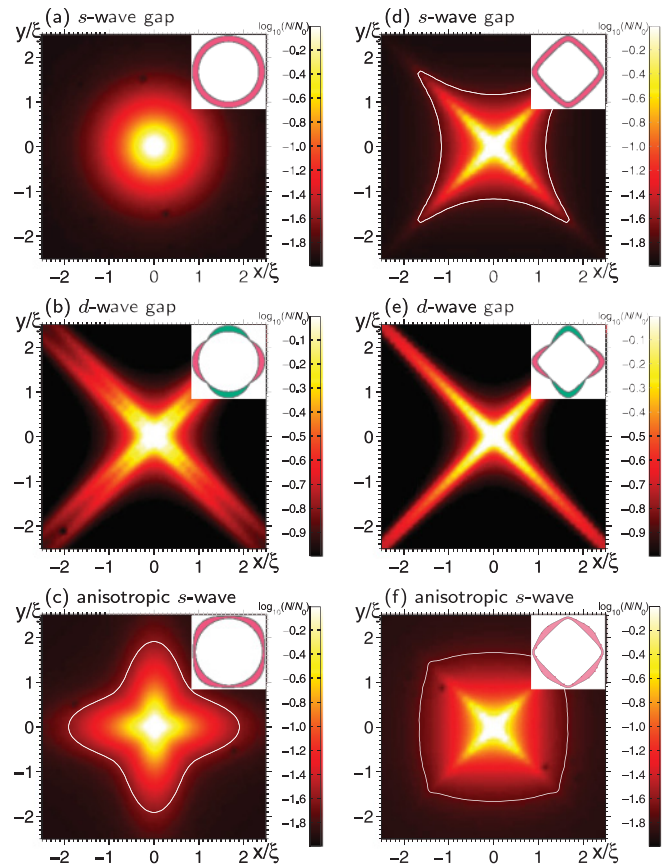


FIG. 2. (Color online) Normalized ZDOS in a $2.5\xi_0 \times 2.5\xi_0$ region around the center of the single vortex for different gap models with a circular Fermi surface (a)–(c) and LiFeAs γ pocket (d)–(f): (a), (d) An isotropic s -wave gap Δ_0 ; (b), (e) a nodal d -wave gap $\Delta_0\sqrt{2}\cos 2\theta$; (c), (f) extended s -wave gap $\Delta_0(1 - r\cos 4\theta)/\sqrt{1+r^2/2}$, $r = 0.3$. The gap bulk value is taken to be $\Delta_0 = 1.76T_c$. The inset on each panel represents a cartoon of the corresponding gap along the Fermi surface. White contour lines shown correspond to $0.025N_0$.

the Fermi-surface effects. Now that the basic structure of this competition in the case of the ZDOS has been understood, it is interesting to ask what may happen in the case of finite energies $\omega \neq 0$. Figure 3 shows the calculated LDOS $N(\mathbf{r}, \omega)$ as a function of energy at the vortex core center [Figs. 3(a)–3(c)] and one coherence length away from the center in the 0° direction [Figs. 3(d)–3(f)] and 45° direction [Figs. 3(g)–3(i)]. The spectrum is quite insensitive to the Fermi-surface shape at the vortex core center where the results for the circular FS and LiFeAs γ pocket are almost the same. Away from the vortex center the direction-dependent LDOS $N(\mathbf{r}, \omega = 0)$ reflects the competition between gap and Fermi-surface anisotropy. The higher (lower) LDOS of the LiFeAs γ pocket (circular FS) at zero energy in Fig. 3(i) than that in Fig. 3(f) is equivalent to our result shown in Fig. 2. The quasiclassical theory incorporates the FS properties solely via \mathbf{v}_F , and thus does not account for the possible changes in the shape of the constant energy surfaces for STS biases away from zero. Provided the band shape varies very slowly on the scale of T_c , this neglect should not significantly affect the shape of vortex bound states at nonzero energy, however. On the other hand, even within

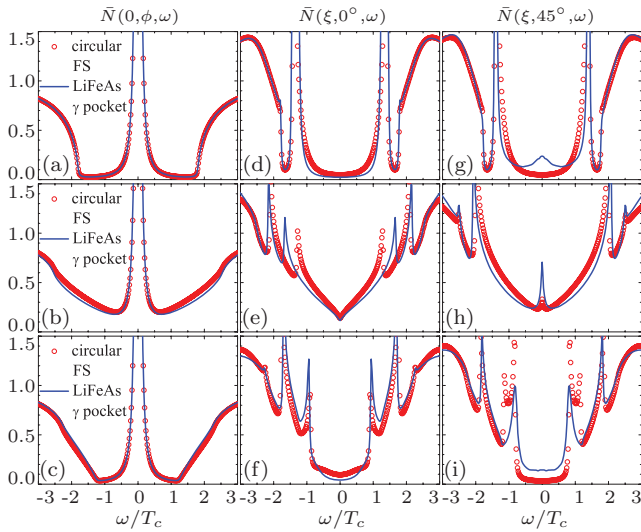


FIG. 3. (Color online) Normalized LDOS $N(\mathbf{r}, \omega)/N_0 \equiv \bar{N}(\rho, \phi, \omega)$ vs energy for different gap models with a circular Fermi surface (red/light gray symbols) and LiFeAs γ pocket (blue/dark gray line): (a), (d), (g) isotropic s -wave gap Δ_0 ; (b), (e), (h) nodal d -wave gap $\Delta_0\sqrt{2}\cos 2\theta$; (c), (f), (i) extended s -wave gap $\Delta_0(1 - r \cos 4\theta)/\sqrt{1 + r^2/2}$, $r = 0.3$. The gap bulk value is taken to be $\Delta_0 = 1.76T_c$. $\mathbf{r} = (\rho, \phi) = (0, \phi)$ for (a)–(c), $(\xi, 0^\circ)$ for (d)–(f), and $(\xi, 45^\circ)$ for (g)–(i).

the current model, a more important effect may be included. In our analysis of LiFeAs, we have until now neglected all Fermi-surface pockets except the outer (γ) hole pocket, due to its square shape and because it seems likely to have the smallest gap. When the bias is increased, higher-energy quasiparticle states, including those associated with larger gaps, will be probed. Within spin fluctuation theory,⁵ both the high density

of states α_2 pocket, and the electron pockets, tend to have gap minima along the 0° directions. Thus as higher energies are probed, it is possible that *rotations* of the bound-state shape may take place as the balance between the gap structure and Fermi-surface anisotropy is altered. Unfortunately, even qualitative statements depend on the details of the sizes of gaps and gap anisotropies on each sheet, as well as on the various Fermi velocities for each band. The LiFeAs system is quite clean, however, and if the current controversy between ARPES²³ and dHvA²⁴ regarding the Fermi surface can be resolved, spectroscopies of bound states on this system should provide enough information to determine a fairly detailed structure of the gap.

Conclusions. We have used quasiclassical methods to calculate the vortex bound states within a single vortex approximation, and highlighted the competition between gap and Fermi-surface anisotropy in the determination of the shape of STS images of vortex bound states. If the Fermi-surface anisotropy is large enough, we have shown that the tails of vortex bound states at low energy need not correspond to the smallest gaps in the system, if those gaps are not true nodes. The ZDOS shape measured by STS in experiments on the LiFeAs system with very clean surfaces is well reproduced by numerical calculation. Within our model, we attribute the tail-like spectrum to the effect of the nonuniform distribution of the Fermi velocity direction on the Fermi surface of the LiFeAs γ hole pocket. Further measurements of the energy dependence of the bound-state shape may further help identify the gap anisotropy.

Acknowledgment. The authors are grateful to T. Hanaguri and J. C. Davis for useful discussions. Y.W. and P.J.H. were supported by the DOE under Grant No. DE-FG02-05ER46236, and I.V. under Grant No. DE-FG02-08ER46492.

¹Y. Kamihara, T. Watanabe, M. Hirano, and H. Hosono, *J. Am Chem. Soc.* **130**, 3296 (2008).
²F. Hsu, J. Luo, K. Yeh, T. Chen, T. Huang, P. Wu, Y. Lee, Y. Huang, Y. Chu, D. Yan *et al.*, *Proc. Natl. Acad. Sci. USA* **105**, 14262 (2008).
³H. Wen, *Annu. Rev. Condens. Matter Phys.* **2**, 121 (2011).
⁴G. Stewart, *Rev. Mod. Phys.* **83**, 1589 (2011).
⁵P. J. Hirschfeld, M. Korshunov, and I. I. Mazin, *Rep. Prog. Phys.* **74**, 124508 (2011).
⁶A. Kemper, T. Maier, S. Graser, H. Cheng, P. Hirschfeld, and D. Scalapino, *New J. Phys.* **12**, 073030 (2010).
⁷Y. Matsuda, K. Izawa, and I. Vekhter, *J. Phys. Condens. Matter* **18**, R705 (2006).
⁸S. Graser, G. R. Boyd, C. Cao, H.-P. Cheng, P. Hirschfeld, and D. Scalapino, *Phys. Rev. B* **77**, 180514 (2008).
⁹B. Zeng, G. Mu, H. Luo, T. Xiang, I. Mazin, H. Yang, L. Shan, C. Ren, P. Dai, and H.-H. Wen, *Nat. Commun.* **1**, 112 (2010).
¹⁰M. Yamashita, Y. Senshu, T. Shibauchi, S. Kasahara, K. Hashimoto, D. Watanabe, H. Ikeda, T. Terashima, I. Vekhter, A. B. Vorontsov, and Y. Matsuda, *Phys. Rev. B* **84**, 060507 (2011).
¹¹A. B. Vorontsov and I. Vekhter, *Phys. Rev. Lett.* **105**, 187004 (2010).

¹²A. V. Chubukov and I. Eremin, *Phys. Rev. B* **82**, 060504 (2010).
¹³J. M. Byers, M. E. Flatté, and D. J. Scalapino, *Phys. Rev. Lett.* **71**, 3363 (1993).
¹⁴A. V. Balatsky, I. Vekhter, and J.-X. Zhu, *Rev. Mod. Phys.* **78**, 373 (2006).
¹⁵O. Fischer, M. Kugler, I. Maggio-Aprile, C. Berthod, and C. Renner, *Rev. Mod. Phys.* **79**, 353 (2007).
¹⁶J.-X. Zhu and C. S. Ting, *Phys. Rev. Lett.* **87**, 147002 (2001).
¹⁷H. F. Hess, R. B. Robinson, and J. V. Waszczak, *Phys. Rev. Lett.* **64**, 2711 (1990).
¹⁸N. Hayashi, M. Ichioka, and K. Machida, *Phys. Rev. Lett.* **77**, 4074 (1996).
¹⁹X. Hu, C. S. Ting, and J.-X. Zhu, *Phys. Rev. B* **80**, 014523 (2009).
²⁰D. Wang, J. Xu, Y.-Y. Xiang, and Q.-H. Wang, *Phys. Rev. B* **82**, 184519 (2010).
²¹Y. Yin, M. Zech, T. L. Williams, X. F. Wang, G. Wu, X. H. Chen, and J. E. Hoffman, *Phys. Rev. Lett.* **102**, 097002 (2009); L. Shan, Y. Wang, B. Shen, B. Zeng, Y. Huang, A. Li, D. Wang, H. Yang, C. Ren, Q. Wang *et al.*, *Nat. Phys.* **7**, 325 (2011).
²²D. J. Singh, *Phys. Rev. B* **78**, 094511 (2008).

- ²³S. V. Borisenko, V. B. Zabolotnyy, D. V. Evtushinsky, T. K. Kim, I. V. Morozov, A. N. Yaresko, A. A. Kordyuk, G. Behr, A. Vasiliev, R. Follath, and B. Büchner, *Phys. Rev. Lett.* **105**, 067002 (2010).
- ²⁴C. Putzke, A. Coldea, I. Guillamon, D. Vignolles, A. McCollam, D. LeBoeuf, M. Watson, I. Mazin, S. Kasahara, T. Terashima, T. Shibauchi, Y. Matsuda, and A. Carrington, e-print [arXiv:1107.4375](https://arxiv.org/abs/1107.4375).
- ²⁵H. Kim, M. A. Tanatar, Y. J. Song, Y. S. Kwon, and R. Prozorov, *Phys. Rev. B* **83**, 100502 (2011).
- ²⁶F. Wei, F. Chen, K. Sasmal, B. Lv, Z. J. Tang, Y. Y. Xue, A. M. Guloy, and C. W. Chu, *Phys. Rev. B* **81**, 134527 (2010).
- ²⁷Y. Wang, J. S. Kim, G. R. Stewart, P. J. Hirschfeld, S. Graser, S. Kasahara, T. Terashima, Y. Matsuda, T. Shibauchi, and I. Vekhter, *Phys. Rev. B* **84**, 184524 (2011).
- ²⁸G. Eilenberger, *Z. Phys.* **214**, 195 (1968).
- ²⁹A. I. Larkin and Y. N. Ovchinnikov, *Sov. Phys. JETP* **28**, 1200 (1969).
- ³⁰J. Serene and D. Rainer, *Phys. Rep.* **101**, 221 (1983).
- ³¹M. Ichioka, N. Hayashi, and K. Machida, *Phys. Rev. B* **55**, 6565 (1997).
- ³²S. Baroni, A. Dal Corso, S. de Gironcoli, P. Giannozzi, C. Cavazzoni, G. Ballabio, S. Scandolo, S. Chiarotti, P. Focher, A. Pasquarello, K. Laasonen, A. Trave, R. Car, N. Marzari, and A. Kokalj, [<http://www.pwscf.org>] (2011).
- ³³S. Graser, A. F. Kemper, T. A. Maier, H.-P. Cheng, P. J. Hirschfeld, and D. J. Scalapino, *Phys. Rev. B* **81**, 214503 (2010).
- ³⁴S. Maiti, M. M. Korshunov, T. A. Maier, P. J. Hirschfeld, and A. V. Chubukov, *Phys. Rev. Lett.* **107**, 147002 (2011).
- ³⁵S. Graser, T. Maier, P. Hirschfeld, and D. Scalapino, *New J. Phys.* **11**, 025016 (2009).
- ³⁶L. Kramer and W. Pesch, *Z. Phys.* **269**, 59 (1974).
- ³⁷W. Pesch and L. Kramer, *J. Low Temp. Phys.* **15**, 367 (1974).
- ³⁸M. Ichioka, N. Hayashi, N. Enomoto, and K. Machida, *Phys. Rev. B* **53**, 15316 (1996).
- ³⁹T. Dahm, S. Graser, C. Iniotakis, and N. Schopohl, *Phys. Rev. B* **66**, 144515 (2002).
- ⁴⁰For a d -wave gap along a circular Fermi surface, near the nodal directions $\theta \approx \frac{\pi}{4}$, the energy spectrum is not strongly restricted to a zero impact parameter. As long as $\theta = \theta_{v_F} \approx \frac{\pi}{4}$, the LDOS is enhanced and therefore this case has wider tails along directions $\phi \approx \frac{\pi}{4}$.
- ⁴¹T. Hanaguri (private communication).